

## Chromic Properties of Dibenzo[*j,l*]fluoranthenes Exhibiting Different Resonance Contribution Based on Cross-conjugation

Kazuma Kurokawa,<sup>a</sup> Naoki Ogawa,<sup>a</sup> Yusuke Kuroda,<sup>a</sup> Yousuke Yamaoka,<sup>a</sup> Hiroshi Takikawa,<sup>a</sup> Kazunori Tsubaki<sup>b</sup> and Kiyosei Takasu<sup>\*a</sup>

<sup>a</sup>Graduate School of Pharmaceutical Sciences, Kyoto University, Yoshida, Sakyo-ku, Kyoto 606-8501, Japan

<sup>b</sup>Graduate School of Life and Environmental Sciences, Kyoto Prefectural University, Shimogamo, Sakyo-ku, Kyoto 606-8522, Japan

**Abstract:** Herein we designed hydroxy-substituted dibenzo[*j,l*]fluoranthenes as novel chromic compounds and evaluated their halochromic properties by UV-vis and fluorescence spectroscopy. Under basic conditions, the 1-hydroxy derivatives show hyperchromic shift, whereas the 9-hydroxy derivatives show bathochromic shift and fluorescence although the skeleton of chromophore is same. Density functional theory (DFT) calculations indicated that the different chromic properties are attributed to the difference in their resonance structures.

Chromism is the reversible colour change that a compound undergoes induced by external stimuli (pH, solvent, heat, light, mechanical stimuli, etc.) and is used for food additive detection,<sup>1</sup> light dimmers,<sup>2</sup> and biological probes.<sup>3</sup> The design strategies of organic chromic molecules are usually based on changes in the  $\pi$ -conjugation<sup>3a,4</sup> or molecular aggregation of long linearly conjugated molecules.<sup>5</sup> Polycyclic aromatic hydrocarbons (PAHs) have also attracted considerable attention as chromophores because of their expected absorption in the visible and near-infrared regions.<sup>6</sup> Fluoranthenes, whose skeleton contains benzene and naphthalene units connected by a cyclopentane ring, represent a class of non-alternant PAHs. Fluoranthenes are found not only in incomplete combustion products as pollutants,<sup>7</sup> but also in nature as biologically active compounds.<sup>8</sup> The fluoranthene core is also utilised as a chromophore in materials science. Fluoranthene derivatives have been developed for use in fluorescent sensors,<sup>9</sup> optoelectronic devices,<sup>10</sup> and dye-sensitised solar cells.<sup>11</sup>

Several efforts for the syntheses of fluoranthene derivatives have been reported,<sup>12</sup> and recently we have also achieved the synthesis of  $\pi$ -extended fluoranthenes by a domino reaction (Scheme 1).<sup>13</sup> Thus, a reaction of biaryl compound **1a** bearing acyl and naphthylalkenyl moieties with KHMDS afforded 1-hydroxydibenzo[*j,l*]fluoranthenes **2a** via (2+2) cycloaddition– $S_NAr$ –*O,C* migration–retro (2+2)

cycloaddition sequence. In the course of our study, to clarify the properties of the synthetic compounds, we found that the UV-vis absorbance of **2a** changed reversibly depending on the pH of the solution (halochromism). This colour change may have resulted from the various possible resonance structures owing to the cross-conjugation of the two aromatic systems of the fluoranthene skeleton. We envisaged that the introduction of an auxochrome, such as a hydroxy group, at the appropriate position in the chromophore would induce characteristic chromic properties depending on the resulting resonance hybrid. We designed two types of hydroxy-substituted dibenzo[*j,l*]fluoranthenes, with substitutions at positions 1 and 9, viz. **2a–c** and **3a–c**, respectively. We expected that the resonance contribution could be controlled by adjusting the position of the hydroxy substituent. Thus, the contribution of the fluorenyl-type structure increased in the anion of **2**, whereas that of the quinoid-type resonance increased in the anion of **3** (Figure 1). Herein, we report the syntheses and photophysical properties of dibenzo[*j,l*]fluoranthenes bearing a hydroxy group, which exhibit halochromism in their UV-vis absorption and fluorescence spectra based on changes in their  $\pi$ -conjugation states.

As a representative procedure, the synthetic route for **3a** is illustrated in Scheme 2. In accordance with our previous report, 1-hydroxy-9-methoxydibenzo[*j,l*]fluoranthene (**2b**) was synthesised from the corresponding biaryl ketone **1b**. After triflation of **2b**, Pd-catalysed reduction of the resulted **5** in the presence of Et<sub>3</sub>SiH, followed by demethylation using BBr<sub>3</sub>, afforded 9-hydroxyfluoranthene **3a**. Compounds **2c** and **3b,c** were also synthesised from the common substrate **2b**. Methyl ether **4** was also prepared from **2a**.

The chromic properties of hydroxyfluoranthenes **2a** and **3a** were analysed by UV-vis and fluorescence spectroscopy under neutral, basic, and acidic conditions in CH<sub>2</sub>Cl<sub>2</sub> solution (Figure 2). The absorption spectrum of 1-hydroxy **2a** exhibited two major bands at 400 nm (moderate) and 420–500 nm (broad, weak) under neutral conditions (Figure 2a). When 1,8-diazabicyclo[5.4.0]undec-7-ene (DBU) was titrated with **2a**, the absorption at 450 nm gradually increased and became saturated with the addition of 1.0 equivalent of DBU. In contrast, no chromic changes were observed when excess trifluoroacetic acid (TFA) was added. The emission spectrum of **2a** shows yellow-green fluorescence at 537 nm ( $\lambda_{\text{ex}} = 381$  nm) under neutral conditions (Figure 2b). When DBU was added to the solution of **2a**, the fluorescence was dramatically strengthened at almost the same wavelength. Reversible photophysical changes in **2a** with DBU were observed upon the addition of acid. The hyperchromic property of **2a** is induced by deprotonation of the phenolic proton. It was clearly proved that almost the same absorption spectra was observed for methyl ether **4** both in the absence or presence of DBU or TFA (Figure 2c). Interestingly, the chromic properties of 9-hydroxy derivative **3a** were different from those of 1-hydroxy derivative **2a**. Although **3a** exhibits major bands at 400 nm (moderate) and 410–530 nm (broad, weak) under neutral and acidic conditions, respectively, the absorption at longer wavelengths is red-shifted to 420–630 nm upon titration with DBU. The bathochromic shift was saturated with the addition of 30 equivalents of DBU (Figure 2d). The colour of the solution turned

red under basic conditions. The emission of **3a** was observed at 571 nm under neutral conditions ( $\lambda_{\text{ex}} = 381$  nm). Upon the addition of DBU (30 equiv.),<sup>‡</sup> emission at longer wavelength (715 nm) was observed albeit weak (Figure 2e).

The effects of substitution on the halochromism of **2** and **3** were also elucidated (Figure 3 and Table 1). The series of 1-hydroxy compounds **2** exhibited similar absorption spectra and hyperchromic properties, independent of the substitution of electron-donating (**2b**) or electron-withdrawing (**2c**) groups at the 9 position (Figure 3a). In contrast, for the series of 9-hydroxy derivatives **3c**, presence of an electron-withdrawing group at the 1 position leads to absorption at longer wavelengths than **3a** and **3b**. A bathochromic shift of **3** was observed upon the addition of DBU (Figure 3b). Notably, 1-cyano-9-hydroxy **3c** exhibited absorption red-shifted by more than 100 nm and near-infrared fluorescence ( $\lambda_{\text{em}} = 764$  nm,  $\lambda_{\text{ex}} = 365$  nm) under basic conditions. Interestingly, comparing the donor- $\pi$ -acceptor type molecules **2c** and **3c**, the introduction of the CN group at the 9 position of 1-hydroxydibenzofluoranthene (**2c**) had little effect on the absorption and fluorescence, while the introduction of this electron-withdrawing group at the 1 position of the 9-hydroxy group (**3c**) resulted in a significant bathochromic shift.

To gain insight into the electron density, transition energy, and oscillator strength of **2** and **3**, time-dependent density functional theory (TD-DFT) calculations were performed (Figure 4a). The calculations predict that the neutral and anionic forms of **2a** show absorption bands assigned to HOMO–LUMO transitions at  $\lambda_{\text{cal}} = 455$  and 454 nm with oscillator strengths ( $f$ ) of 0.0904 and 0.1726, respectively. These results were consistent with the experimentally observed hyperchromic effects of **2a**. These results were consistent with the experimentally observed hyperchromic effects of **2a**. The TD-DFT calculations also predicted a bathochromic shift in **3a**. While the neutral and anionic forms of **3a** show broad absorption at 410–530 nm and 420–630 nm, respectively, the HOMO–LUMO transitions are calculated to be  $\lambda_{\text{cal}} = 488$  and 652 nm with  $f$  values of 0.1726 and 0.1803, respectively.

Nucleus-independent chemical shifts (NICS) were calculated to estimate the local aromaticity of each ring in both the neutral and anionic forms of **2a** and **3a** (Figure 4b). According to the calculations, the pentagonal rings (ring D) of the neutral and anionic forms of **2a** show NICS(1) values of +0.18 and –6.03, respectively, implying that the pentagon was converted from non-aromatic to aromatic under basic conditions. The NICS(1) values indicated that the aromaticity of ring F decreased under basic conditions. These results suggest that the anionic form of **2a** makes a large contribution to the fluorenyl-anion-type resonance, as shown in Figure 1. In contrast, the NICS(1) values show that the aromatic characters of the A, B, and F rings of the anionic form of **3a** is weaker than that of the neutral form, and the local antiaromatic character of ring D increases under basic conditions, suggesting that the contribution of quinoid resonance increases under basic conditions. These calculations suggest

that the characteristic chromic properties of **2** and **3** are caused by the different resonance hybrids.

In this study, we synthesised new halochromic fluoranthene derivatives and found that although the same chromophore skeleton was used, changing the position of the auxochromes afforded contrasting halochromic properties under basic conditions. Notably, 9-hydroxydibenzofluoranthenes **3** exhibit emissions red-shifted by almost 200 nm compared to 1-hydroxy compounds **2**. TD-DFT and NICS calculations supported the idea that the characteristic chromic properties of fluoranthenes are based on changes in the resonance structures of the cross-conjugated system.

**Acknowledgements:** This work was supported by JSPS KAKENHI (Grant Number 21K18959) and MEXT KAKENHI (Grant Number JP21H05211) in Digi-TOS and BINDS from AMED (Grant Numbers 22ama121042j0001 and 22ama121034j0001). K.K. acknowledges support from Sasakawa Scientific Research Grant and JST SPRING (JPMJSP2110).

**Conflicts of interest:** There are no conflicts to declare.

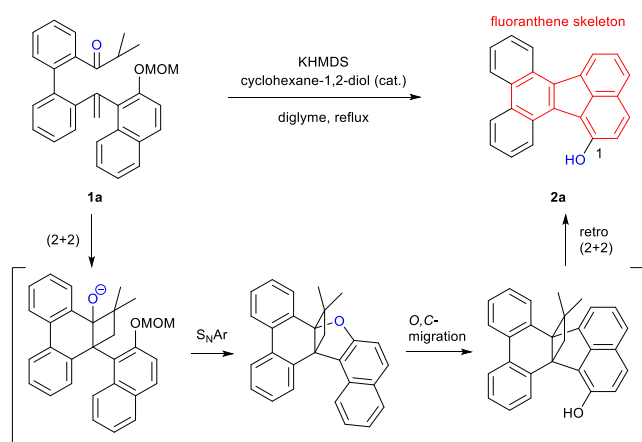
## References

‡ The amount of base required for complete deprotonation depends on the  $pK_a$  value of **2a** ( $12.9 \pm 0.2$  in DMSO) and **3a** ( $14.2 \pm 0.3$  in DMSO).

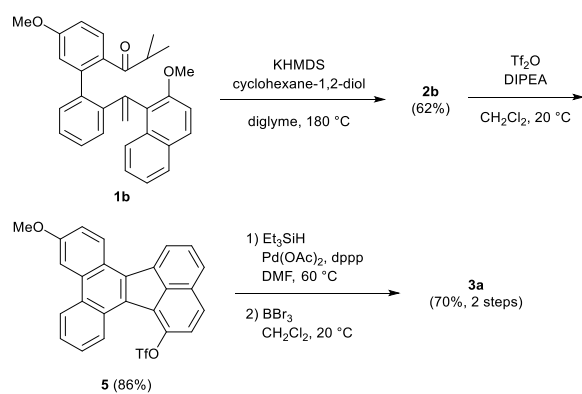
- 1 H. Almasi, S. Forghani and M. Moradi, *Food Packag. Shelf Life*, 2022, **32**, 100839.
- 2 (a) P. R. Somani and S. Radhakrishnan, *Mater. Chem. Phys.*, 2002, **77**, 117. (b) Y. Ke, C. Zhou, Y. Zhou, S. Wang, S. H. Chan and Y. Long, *Adv. Funct. Mater.*, 2018, **28**, 1800113.
- 3 (a) A. Steinegger, O. S. Wolfbeis and S. M. Borisov, *Chem. Rev.*, 2020, **120**, 12357; (b) N. Bar and P. Chowdhury, *ACS Appl. Electron. Mater.*, 2022, **4**, 3749.
- 4 (a) K. Taguchi, *J. Am. Chem. Soc.*, 1986, **108**, 2705. (b) A. Singh, R. Choi, B. Choi and J. Koh, *Dyes Pigm.*, 2012, **95**, 580.
- 5 (a) Y. Dong, J. W. Y. Lam, A. Qin, Z. Li, J. Liu, J. Sun, Y. Dong and B. Z. Tang, *Chem. Phys. Lett.*, 2007, **446**, 124. (b) H. long, D. Guo, L. Wang, Z. Liu, S. Li, X. Liang, Y. Chen, Z. Yang, J. Li, L. Dong and L. Tan, *Dyes Pigm.*, 2022, **203**, 110330.
- 6 (a) G. Laus, H. Schottenberger, K. Wurst, J. Schütz, K. H. Ongania, U. E. I. Horvath and A. Schwärzler, *Org. Biomol. Chem.*, 2003, **1**, 1409; (b) H. Enozawa, S. Ukai, H. Ito, T. Murata and Y. Morita, *Org. Lett.*, 2019, **21**, 2161; (c) W. Chen, S. Liu, Y. Ren, S. Xie, C. Yan, Z. Zhou and G. Zhou, *Chem. Eur. J.*, 2023, **29**, e202203238.

- 7 A. Wetzel, T. Alexander, S. Brandt, R. Haas and D. Werner, *Bull. Environ. Contam. Toxicol.*, 1994, **53**, 856.
- 8 (a) G. Brauers, R. Ebel, R. Edrada, V. Wray, A. Berg, U. Gräfe and P. Proksch, *J. Nat. Prod.*, 2001, **64**, 651; (b) K. Koyama, D. Kuramochi, K. Kinoshita, and K. Takahashi, *J. Nat. Prod.*, 2002, **65**, 1489; (c) L. Du, J. B. King and R. H. Cichewicz, *J. Nat. Prod.*, 2014, **77**, 2454.
- 9 (a) N. Venkatramaiah, S. Kumar and S. Patil, *Chem. Commun.*, 2012, **48**, 5007; (b) A. Goel, A. Sharma, M. Kathuria, A. Bhattacharjee, A. Verma, P. R. Mishra, A. Nazir and K. Mitra, *Org. Lett.*, 2014, **16**, 756; (c) I. Kawajiri, M. Nagahara, H. Ishikawa, Y. Yamamoto, J. Nishida, C. Kitamura and T. Kawase, *Can. J. Chem.*, 2017, **95**, 371; (d) J. Yang, M. Horst, S. H. Werby, L. CegeIski, N. Z. Burns and X. Yang, *J. Am. Chem. Soc.*, 2020, **142**, 14619; (e) W. Shi, X. Yang, X. Li, L. Men, D. Zhang, Z. Zhu, X. Xiao and D. Zhao, *Chem. Eur. J.*, 2022, **28**, e202104598.
- 10 H. Wu, R. Fang, J. Tao, D. Wang, X. Qiao, X. Yang, F. Hartl and H. Li, *Chem. Commun.*, 2017, **53**, 751.
- 11 W. Wu, J. Li, F. Guo, L. Zhang, Y. Long and J. Hua, *Renew. Energ.*, 2010, **35**, 1724.
- 12 (a) C. F. H. Allen and J. A. VanAllan, *J. Org. Chem.*, 1952, **17**, 845; (b) M. Yamaguchi, M. Higuchi, K. Tazawa and K. Manabe, *J. Org. Chem.*, 2016, **81**, 3967; (c) J. Karunakaran and A. K. Mohanakrishnan, *Eur. J. Org. Chem.*, 2017, 6747; (d) S. Pal, Ö. Metin and Y. E. Türkmen, *ACS Omega*, 2017, **2**, 8689; (e) H. Takano, N. Shiozawa, Y. Imai, K. S. Kanyiva and T. Shibata, *J. Am. Chem. Soc.*, 2020, **142**, 4714; (f) S. Yang and Y. Zhang, *Org. Lett.*, 2022, **24**, 9060.
- 13 N. Ogawa, Y. Yamaoka, K. Yamada, K. and K. Takasu, *Org. Lett.*, 2017, **19**, 3327.
- 14 C. A. Parker and W. Rees, *Analyst*, 1960, **85**, 587.

## Artworks



**Scheme 1.** A domino reaction giving dibenzofluoranthene **2a**



**Scheme 2.** Preparation of **3a** as a typical synthetic procedure.

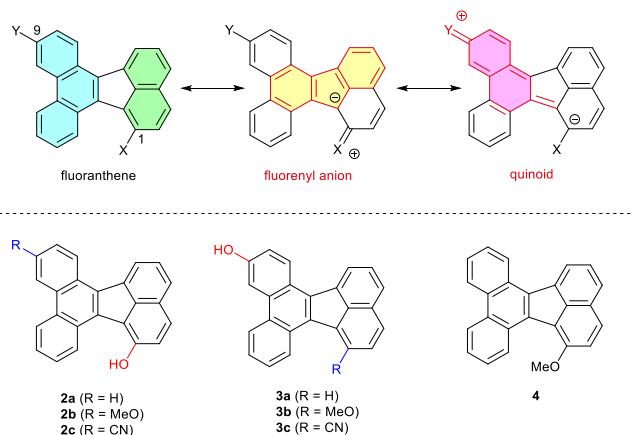


**Figure 1.** Typical resonance structures of dibenzofluoranthene and designed dibenzo[*j,k*]fluoranthenes **2a–c**, **3a–c** and **4**

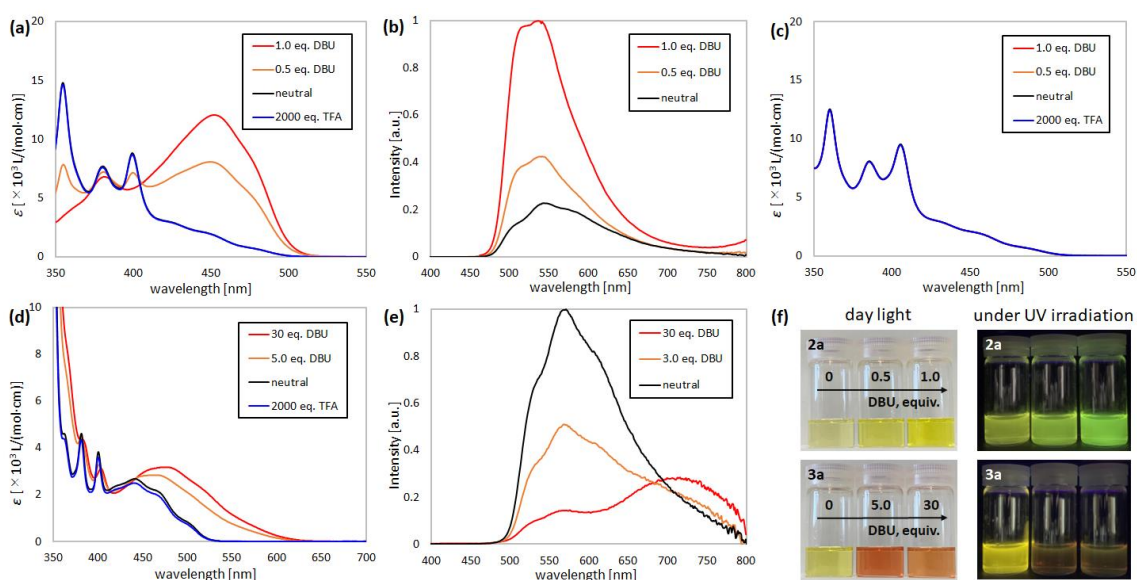


**Figure 2.** UV-vis absorption spectra of (a) **2a**, (c) **4** and (d) **3a** in  $\text{CH}_2\text{Cl}_2$ , titrated with DBU or TFA at 296 K. Emission spectra of (b) **2a** and (e) **3a** in  $\text{CH}_2\text{Cl}_2$ , titrated with DBU at 296 K. (f) The colour change of **2a** (above) and **3a** (bottom) under neutral or basic conditions.

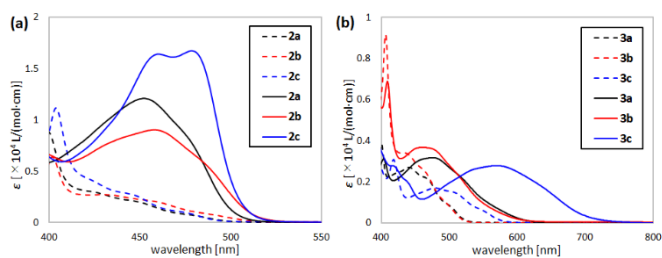


**Figure 3.** UV-vis absorption spectra of (a) **2a–c** and (b) **3a–c** without additive (dashed lines) and with DBU (solid lines) in  $\text{CH}_2\text{Cl}_2$  at 296 K.

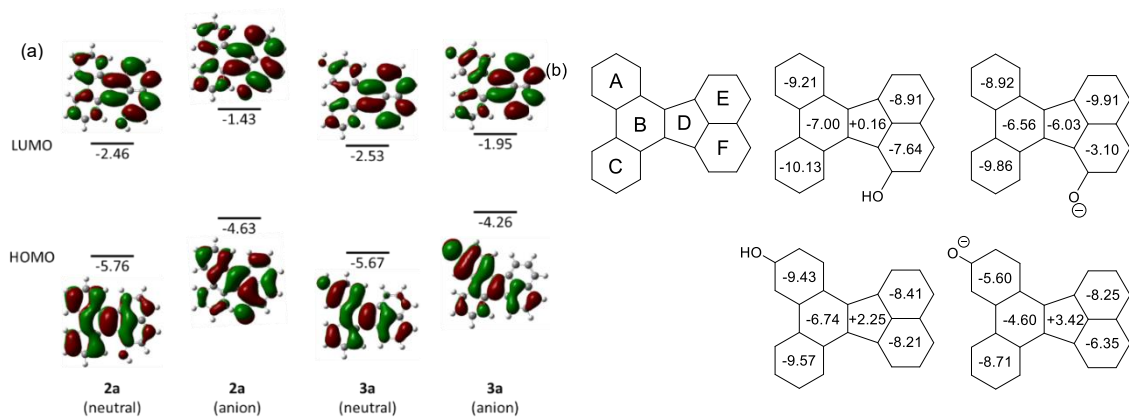


**Figure 4.** (a) Calculated frontier molecular orbitals and energy levels of **2a** (neutral, anion) and **3a** (neutral, anion) at the TD-B3LYP/6-311+G(d,p)-CPCM(DCM). (b) NICS(1) values of **2a** (neutral, anion) and **3a** (neutral, anion) at the GIAO/B3LYP/6-311+G(d,p).

**Table 1.** Photophysical properties of the hydroxy-dibenzofluoranthenes **2** and **3** in CH<sub>2</sub>Cl<sub>2</sub>.<sup>a</sup>

Compounds	Neutral form (no additive)			Anionic form (in the presence of DBU) <sup>b</sup>		
	$\lambda_{\text{Abs.}}$ [nm] ( $\epsilon$ [ $10^3$ L/(mol cm)])	$\lambda_{\text{Em.}}$ [nm]	$\Phi$ [%] <sup>c</sup>	$\lambda_{\text{Abs.}}$ [nm] ( $\epsilon$ [ $10^3$ L/(mol cm)])	$\lambda_{\text{Em.}}$ [nm]	$\Phi$ [%] <sup>c</sup>
<b>2a</b>	400 (8.84), 451 (1.92)	543	3.9	452 (12.1)	537	8.7
<b>2b</b>	402 (6.40), 461 (2.00)	565	3.9	458 (9.00)	554	8.9
<b>2c</b>	404 (11.1), 450 (2.44)	535	6.3	478 (16.7)	511	10
<b>3a</b>	400 (3.84), 442 (2.68)	571	2.7	475 (3.18)	715	0.92
<b>3b</b>	407 (9.16), 440 (3.34)	572	2.8	462 (3.66)	725	1.5
<b>3c</b>	418 (3.08), 480 (1.70)	640	0.57	570 (2.78)	764	0.30

a) Both absorption and emission spectra were recorded in solution at room temperature at  $c = 5.0 \times 10^{-5}$  M. b) Each hydroxy-dibenzofluoranthene (anionic form) was studied in the presence of DBU (for **2a–c**: 1.0 eq.; **3a**: 30 eq.; **3b**: 100 eq.; **3c**: 40 eq.) c) Quinine sulfate was used as reference dye ( $\lambda_{\text{ex}} = 366$  nm,  $\Phi = 55\%$ ).<sup>14</sup>